Arabian Journal of Chemistry (2022) **15**, 103579

King Saud University

Arabian Journal of Chemistry

www.ksu.edu.sa
www.sciencedirect.com

ORIGINAL ARTICLE

Formulation, characterization and biological evaluation of injectable nanocrystals from stem exudate gel of *Caralluma retrospiciens* (Ehrenb) – Part C

Muhammad H. Sultan [a], Sivakumar S. Moni [a,*], Saad S. Alqahtani [b], Hafiz A. Makeen [b,*], Osama A. Madkhali [a], Mohammed Ali Bakkari [a], Santhosh Joseph Menachery [b], Yosif Almoshari [a], Ahmad Salawi [a], Meshal Alshamrani [a], Awaji Y. Safhi [a], Syam Mohan [c], Mohamed Eltaib Elmobark [a]

[a] *Department of Pharmaceutics, Faculty of Pharmacy, Jazan University, Jazan, Saudi Arabia*
[b] *Pharmacy Practice Research Unit, Clinical Pharmacy Department, Faculty of Pharmacy, Jazan University, Jazan, Saudi Arabia*
[c] *Substance Abuse and Toxicology Research Centre, Jazan University, Jazan, Saudi Arabia*

Received 9 September 2021; accepted 15 November 2021
Available online 22 November 2021

KEYWORDS

Nanocrystals;
Exudate gel;
Desert plant;
Caralluma retrospiciens;
Antibacterial properties

Abstract The purpose of this study was to develop injectable nanocrystals (NC) from stem exudate gel (EG) from *Caralluma retrospiciens (Ehrenb)* using the technique of nanoprecipitation. The NC had a zeta potential of −5.58 ± 4.27 mV. Size distribution analysis showed that it ranged in size from 100 to 300 nm. The polydispersity index (PDI) was 0.467, while its percentage PDI was 68.4. Scanning electron microscopic analysis and transmission electron microscopy studies revealed the morphological features of NC as discrete crystals with rough surfaces. The mobility of NC was 5.5 µm.cm/Vs, while its conductivity was 0.16 mS/cm. Antibacterial studies showed broad activity against both Gram-positive and Gram-negative bacteria. The minimum inhibitory concentrations (MICs) of NC against *Bacillus subtilis (B. subtilis)*, *Staphylococcus aureus (S. aureus)*, *Streptococcus pyogenes (S. pyogenes)*, *Escherichia coli (E. coli)*, *Pseudomonas aeruginosa (P. aeruginosa)* and *Klebsiella pneumoniae (K. pneumoniae)* were 6, 8, 8, 4, 8, and 6 % (w/v), respectively. The antibacterial effect was highest against *K. pneumoniae* (25.6 ± 1.5 mm), followed by *E. coli* (25.5 ± 1.8 mm), *P. aeruginosa* (24.1 ± 1.2 mm), *S. pyogenes* (22.2 ± 1.2 mm), *S. aureus* (21.83 ± 1.2 mm)

* Corresponding authors.
E-mail addresses: drsmsivakumar@gmail.com (S.S. Moni), hafiz@jazanu.edu.sa (H.A. Makeen).

Peer review under responsibility of King Saud University.

Production and hosting by Elsevier

https://doi.org/10.1016/j.arabjc.2021.103579

and *B. subtilis* (20.33 ± 1.8 mm). In this study, the cytotoxicity properties of NC were determined against MCF-7 breast cancer cells ATCC. The NC failed to inhibit the proliferation of MCF-7 cells against the even at 300 μg/mL concentration. These results indicated that the NC is a promising antibacterial injectable dosage form.

1. Introduction

Secondary metabolites are among the most abundant sources of bioactive compounds with a high degree of molecular diversity and intriguing pharmacological properties. Traditional medical systems apply natural therapies for a variety of diseases through the use of herbs. The therapeutic potential of medicinal plants has been established all over the world, and they have been widely used for long in various cultures (Ghulam et al., 2015). The use-fulness of herbs in the development of numerous novel medicinal compounds have been documented (Alghamdi et al., 2018; Hosseinkhani et al., 2017; Saad et al., 2020). The Kingdom of Saudi Arabia features a diverse range of flora consisting of many species of trees, herbs, and shrubs, (Aati et al., 2019). The plant *C. retrospiciens* is a desert species that grows in the hilly and semi-desert regions of Saudi Arabia. The EG from the plant has traditionally been used for wound healing by the inhabitants of Saudi Arabia, according to tradition (Makeen et al., 2020).

Nanoparticle drug delivery systems improve the treatment of human diseases through precise delivery of medicines to specific locations within the body, thereby reducing drug doses used, improving pharmacokinetic profile, and reducing drug toxicity (Patra et al., 2018; Wided et al., 2021). The use of herbal nanoparticles is emerging as a unique strategy for developing a better delivery system that enhances the efficacy of biomolecules, penetrates cell membranes, and elicits a spectrum of activities. The design and development of herbal nanoparticles has emerged as a cutting-edge research area in nano formulation. The current study sought to prepare nanocrystals from the EG of *C. retrospiciens*, in continuation of a previous research. The physical characteristics and antibacterial properties of NC were also investigated in this study (Makeen et al., 2020).

2. Materials and methods

2.1. Collection of plant and exudate gel

A sample of the plant was obtained from the hilly region of Rijal Alma, Asir province, Saudi Arabia. The plant sample was transported to the laboratory in perforated polyethylene bags. The stem portions were rinsed several times with ordinary water, and then with Millipore water to eliminate contaminants, followed by airdrying. Identification of the sample was done by a taxonomist, and the plant was identified as *Caralluma retrospiciens* (Ehrenb) N.E.Br belongs to the family belong to the Apocynaceae family and a sample of the plant (reference number: JAZUH 1623) was deposited in the Jazan University herbarium. The exudate gel was collected by cutting the stem longitudinally using a sterile blade. Then, the viscous gel was collected in a clean sterile beaker by keeping the stem in an inclined position (Fig. 1). The gel was collected in a clean sterile beaker and stored at 2 to 4 °C, prior to processing.

2.2. Preparation of nanocrystals

A simple nanoprecipitation technique was developed for the preparation of nanocrystals (NCs). In this technique, a uniform mixture was obtained by stirring 5 mL of EG with a magnetic stirrer on a hot plate at room temperature for 10 min. A reaction mixture (RM) was prepared by adding 90 % v/v methanol, dropwise, to the EG. The mixture was sonicated at predetermined time spans with a probe sonicator. Thereafter, the RM was subjected to filtration. The filtered RM was suspended in 95 % (v/v) ethanol, stirred at 3000 rpm using a magnetic stirrer and kept overnight (16 h) on a hot plate at 80 °C for complete solvent evaporation and crystal formation. Thereafter, the resultant NC was collected by scrapping from the beaker. The collected NC was preserved at 4 °C before its application in further studies.

2.3. Physical characterization of NC

2.3.1. Dynamic light scattering (DLS) analysis

The surface charge of the NC was determined using a zeta potential (ZP) study, followed by, determination of PDI and particle size using DLS technique (Malvern Instruments, UK). The electric conductivity was also measured and expressed in milli Siemens per centimeter (mS/cm). The measurements were done with 1% (w/v) solution of NC after prior filtration.

2.3.2. Assessment of morphology of NC

2.3.2.1. SEM and EDAX analysis (Moni et al., 2018). The morphological features of NS nanocrystals were investigated using a high-power scanning electron microscope. A sample of the crystal NS was placed on metal stubs and plated with a film of gold–palladium 200–300 Å thick at lowered pressure. The SEM analysis of NS was studied at different magnifications. Energy Dispersive Spectroscopy (EDAX) is a useful technique for determining the elemental compositions of crystals. The EDAX spectrum was obtained at an acceleration voltage of 5 keV and collected at 31 s.

2.3.2.2. Transmission electron microscopy. Transmission Electron Microscopy (TEM) is a technique that produces images of nano-particles with extremely high spatial and temporal resolution. The NC sample [1 % (w/v) in Millipore water] was subjected to characterization using a JEOL TEM (Japan) in line with the procedure described previously (Osama et al., 2021).

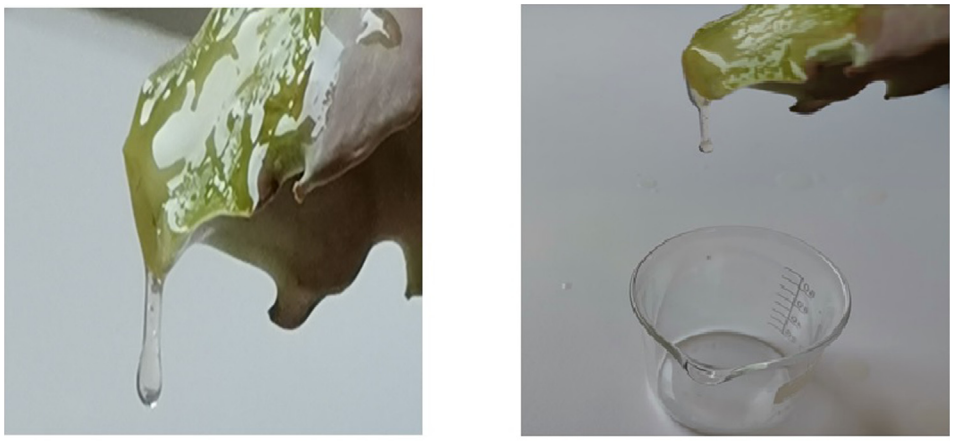

Fig. 1 Collection of the exudate gel (EG) from the stem of *Caralluma retrospiciens*.

2.4. ***Determination of antibacterial effect of NC*** *(Moni et al., 2018)*

2.4.1. Standardization of working stock culture

Human pathogenic bacteria *Bacillus subtilis*, *Staphylococcus aureus*, *Streptococcus pyogenes*, *Escherichia coli*, *Pseudomonas aeruginosa*, and *Klebsiella pneumoniae* were employed in this study. Sub-cultures were prepared in nutrient broth, from stock cultures of the organisms. The subcultures were incubated for 24 h at 37 °C, and were serially diluted with nutrient broth, with an initial dilution done with Millipore water. The potential viability of the bacterial organisms was measured in terms of CFU per mL. The MIC and antibacterial action of NC were determined using a standardized culture.

2.4.2. Determination of minimum inhibitory concentration (MIC)

The broth tube dilution method was used to determine MIC. Pre-determined concentrations of NC [1, 2, 4, 6, 8 and 10 % (w/v)] were prepared by dilution in nutrient broth. The MIC was determined based on the visibility of bacterial growth in the broth.

2.4.3. Determination of antibacterial susceptibility

The concentration of NC used was selected based on the MIC study to determine antibacterial susceptibility of each of the tested bacterial species. The antibacterial investigation was carried out using Muller Hinton (MH) agar plates. Antibacterial tests were performed on the bacterial cultures using the spread plate technique, with ciprofloxacin as standard drug (Cappuccino and Sherman, 2014). The agar wells were 10 mm in diameter, and NCs and ciprofloxacin standard were put in different wells of a plate. The measurement of antibacterial effect was based on the formation of areas of growth inhibition following 24 h culturing at 37 °C. The diameter of zone of inhibition was measured and recorded, since it is directly related to the antibacterial activity.

2.5. Cytotoxic effect

The human breast cancer cells MCF-7 were cultured and maintained in RPMI-1640 medium which contain sodium bicarbonate buffer system (2.0 g/L) at pH 7.4. The media were supplemented with 10% Fetal Bovine Serum (FBS), penicillin (100 U/**mL**), streptomycin (100 µ**g / mL**), and cells were grown individually in a CO_2 incubator (Heraeus, Germany) at 37 °C with 90% humidity and 5% CO_2. The cytotoxicity properties of NC were performed as reported earlier (Sultan et al., 2020). In this study, gradient concentration of nanocrystals 25, 50, 100, 150, 200 µg/mL were screened to find out cytotoxicity effect.

2.5.1. Statistical analysis

Statistical analysis was performed by using Graph pad Prism software (Version 8.3.1), USA through one-way analysis of variance (ANOVA), followed by Tukey Kramer analysis as a post-hoc test.

3. Results

3.1. Physical characterization

3.1.1. Exudate gel (EG)

Fig. 1 demonstrates the collection of EG from the stem of *C. retrospiciens*. The colour of EG was pale yellow, and it had a thick and uniform consistency, with a textural **smoothness** that was uniform and consistent.

3.1.2. DLS analysis

The physical characteristics of the NCs are presented in Table 1. From the study, it was revealed that the NCs exhibited a zeta potential of −5.58 ± 4.27 mV. The PDI value of NCs was 0.467, with 68.4 % polydispersity, indicating that the nanocrystal formulation was not significantly stable with good uniform particle distribution. The zeta size of NCs was

Table 1 Physical characterization of NC.

Zeta potential (mV)	Conductivity (mS/cm)	PDI	% Poly dispersity	NC size (z d.nm)	NC size in mass (r.nm)	% Mass (r. nm)	Mobility (μm.cm/Vs)
−5.58 ± 4.27	0.160	0.467	68.4	101.4	266.4 ± 200.9	2.51	5.5

NC: Nanocrystals; PDI: Poly dispersity index; mV: Milli Volt; mS/cm; Milli Siemens per centimetre.

101.4 z.d.nm, and the NC size by means of mass ranged from 266.4 ± 200.9 r.nm, with % mass of 2.51.

3.1.3. SEM and EDAX analysis

Fig. 2A – 2D demonstrate the morphological characteristics of the NCs, as were revealed through scanning electron microscopy (SEM), and the elemental composition, which was determined through EDAX analysis. Fig. 2A shows the injectable dosage form of NCs at × 2000 magnification. The micrograph reveals largely discrete NCs, but few crystals are clumped together to form sheaths at some areas of micrograph. The NCs were clearly observed, mostly as square-type crystals at × 10,000 magnification (Fig. 2B). Furthermore, when the NCs were examined at × 20,000 magnification (Fig. 2C), they were more discrete and square-shaped, and some were lengthy rods with smooth surfaces. Fig. 2D reveals the EDAX analysis of NC showing that they contained 67.29 % carbon (C), 20.08 % oxygen (O), 7.07 % chlorine (Cl), 3.72 % sodium (Na), 0.19 % magnesium (Mg), 0.66 % sulphur (S), 0.12 % calcium, 0.44 % copper (Cu), and 0.43 % Zinc (Zn).

3.1.4. Morphological features of NCs

The morphological features of NCs which were examined using transmission electron microscopy (TEM), are shown in Fig. 3. at 40,000 × magnification, the NCs appeared as rough, elongated crystals in discrete groups (Fig. 3A), and at 120,000 × magnification, they exhibited irregular shapes with rough surfaces clumped each other. However, few crystals were spherical in shape (Fig. 3B).

3.2. Antibacterial studies of NC

3.2.1. Determination of MIC

Table 2 shows the minimum inhibitory concentrations (MICs) of NCs against selected human pathogenic bacteria. The study showed that MIC varied with individual bacterial organism. It

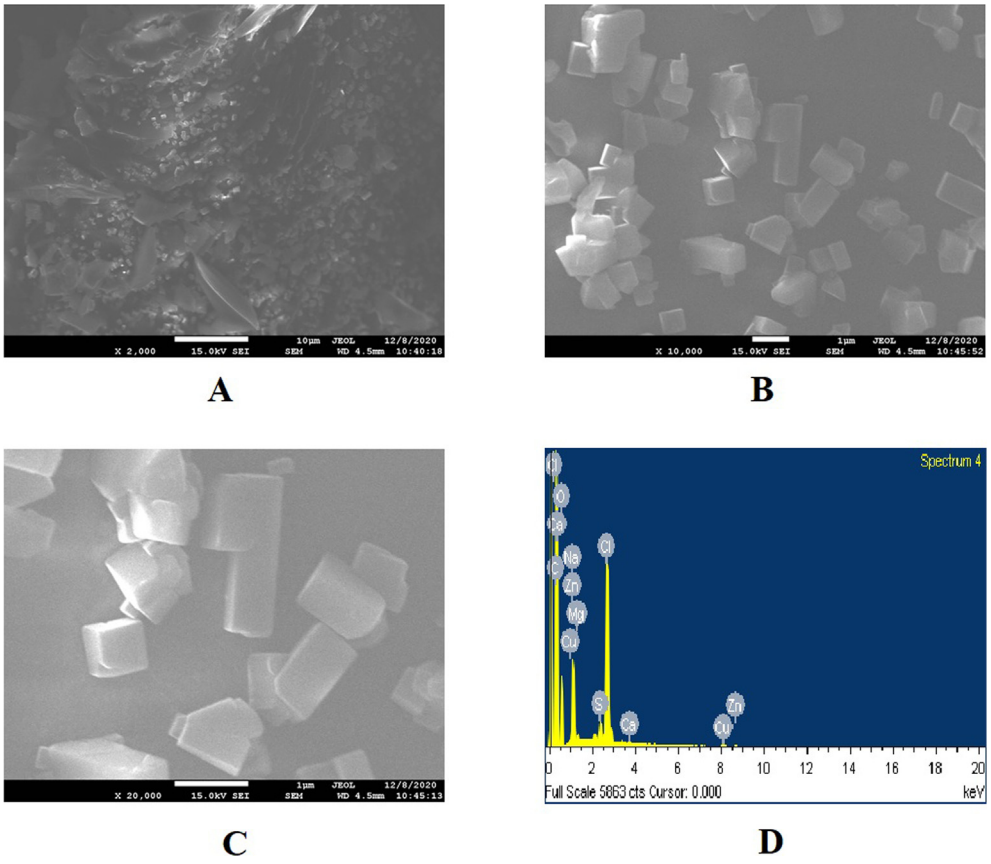

Fig. 2 Scanning Electron Microscopy (SEM) and Energy Dispersive Spectroscopy (EDAX) analysis of Nano crystals (NC). (A) NC at × 2000 Maginification (B) NC at × 10,000 Maginification (C) NC at × 20,000 Maginification (D) EDAX analysis of NC.

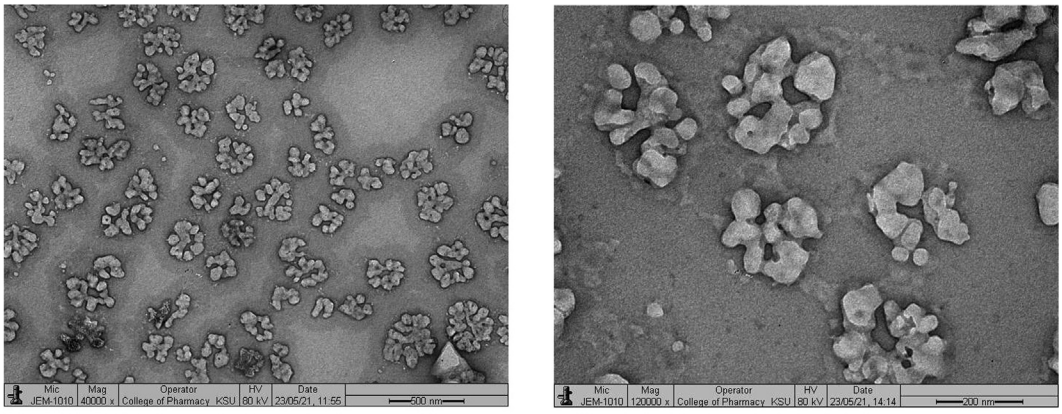

Fig. 3 Transmission electron microscopy (TEM) study. (A) NC at × 40,000 Maginification (B) NC at ×120000 Maginification.

is very obvious that the MIC was 4 % against *E. coli* at a concentration of 3×10^{-5} CFU/mL, followed by *B. subtilis* (6 %) at the concentration of 3×10^{-5} CFU /mL. The MIC of NCs against *K. pneumoniae* was 6 % at the concentration of 3×10^{-3} CFU /mL, while the MIC of NCs against *S. pyogenes* was 8 % at the concentration of 4×10^{-5} CFU/mL. Interestingly, the MICs against *S. aureus* and *P. aeruginosa* were also 8 % at the concentrations of 3×10^{-4} and 3×10^{-3} CFU/mL.

3.2.2. Determination of antibacterial susceptibility

The NCs exerted effective antibacterial action against the microorganisms tested (Table 3). However, the antibacterial effect of NC was a little higher in **Gram**-negative bacteria than in **Gram**-positive bacteria.

3.2.3. Determination of cytotoxicity effect

The NCs did not produce any cytotoxic effect against treated MCF-7 breast cancer cells at a concentration up to 300 µg/mL.

4. Discussion

Resistance to antibiotics develops during standard antibiotic therapy, and it poses a hazard to subsequent treatments of infectious diseases (Ayukekbong et al., 2017). Nature has endowed man with a plethora of plants and shrubs with great potential medicinal values. The Kingdom of Saudi Arabia is rich in rare herbs that have been utilized as folk medicine, but their scientific significance has yet to be discovered. In furtherance of our earlier study (Makeen et al., 2020) the present study reports the potential of NCs prepared from the exudate gel of *C. retrospiciens*. The purpose of developing NC as an injectable nano-formulation was to overcome the stability-related disadvantages, since the exudate gel of *C. retrospiciens* was unstable during storage even at 2 to 8 °C. In the present study, NCs were developed using simple nanoprecipitation technique. The physical qualities of the injectable NCs which reflect their potential, demonstrate that they have good physical properties. The physical characteristics of NCs were unique, when compared to those of the exudate gel.

The ZP of the NCs was −5.58 ± 4.27 mV, whereas the ZP of EG was reported to be − 4.97 mV at 10 % (v/v). Surprisingly, in the earlier investigation, we were unable to determine the ZP at 100 and 50 % EG (v/v) (Makeen et al., 2020). However, the formulated NCs did not have significant ZP but it was better than that of EG, as was observed during experimentation. In contrast, it was possible to determine ZP in NCs prepared from 100 percent EG. The NC formulation exhibited good and acceptable range of ZP. The PDI value of 1% (w/v) NCs was 0.467, and the percent PDI was 68.47, indicating consistency in colloidal injectable formulation. Th polydispersity level was more than 60 %, indicating non-linear monodisperse formulations (Sivakumar et al., 2020). The particle size of the formulated NCs was acceptable, and the zeta size was 101.4 z.d.nm. The pharmacokinetic profile of nanoparticles for biodistribution is determined by their surface charge and particle size. In the present study, the ZP of −5.58 mV is indicative of the potential of the NCs to target bacteria. The

Table 2 Percent minimum inhibitory concentration of sample analyte NC.

Bacterial organisms	Concentration CFU #/mL	Minimum inhibitory concentration (% w/v)					
		1	**2**	**4**	**6**	**8**	**10**
Bacillus subtilis	3×10^{-5}	+	+	+	–	–	–
Staphylococcus aureus	3×10^{-4}	+	+	+	+	–	–
Streptococcus pyogenes	4×10^{-5}	+	+	+	+	–	–
Escherichia coli	3×10^{-5}	+	+	–	–	–	–
Pseudomonas aeruginosa	2×10^{-5}	+	+	+	+	–	–
Klebsiella pneumoniae	3×10^{-3}	+	+	+	–	–	–

NC: Nano crystals; # Colony forming unit**; (+)** Presence of bacterial growth **(-)** Absence of bacterial growth.

Table 3 Antibacterial study of sample analyte NC.

Organisms	Concentration CFU[#]/mL	MIC (% w/v)	Zone of inhibition (mm)	
			NC	**Ciprofloxacin (50 μg/mL)**
Bacillus subtilis	3×10^{-5}	6	20.33 ± 1.8	24.7 ± 1.4*
Staphylococcus aureus	3×10^{-4}	8	21.83 ± 1.2[#ns]	25.8 ± 1.6
Streptococcus pyogenes	4×10^{-5}	8	22.2 ± 1.2[#ns]	26.2 ± 1.5*
Escherichia coli	3×10^{-5}	4	25.5 ± 1.8	27.83 ± 1.2[$ns]
Pseudomonas aeruginosa	2×10^{-5}	8	24.1 ± 1.2	24.5 ± 1.5[$ns]
Klebsiella pneumoniae	3×10^{-3}	6	25.6 ± 1.5	26.8 ± 1.5[$ns]

* Significant when compared to nano crystals at $P < 0.001$, [#]ns**:** non-significant when compared to *Bacillus subtilis* at *P greater than 0.05* treated by nanocrystals; [$ns] non-significant when compared to nanocrystals at *P greater than 0.05*. NC: Nano crystals; MIC: Minimum inhibitory concentration; CFU: Colony forming unit.

mobility of NPs also affects their conductivity. In the present study, high degree of mobility (5.5 μm.cm/Vs) was obtained with 1% (w/v) NCs. An earlier report suggested that injectable sodium selenite nanoparticle exhibited mobility of −3.857 μm. cm/Vs, which was reported as ideal formulation (Sivakumar et al., 2020; Ito et al., 2004). Previous research revealed that particles smaller than 20 nm had high mobilities within colloidal milieu, and also affect surface charge (Ernest et al., 2013). In contrast, NCs of size more than 100 nm exhibit high mobility. Moreover, mobility influences the conductivity of particles. However, the NCs exhibited low conductivity and low % mass (r.nm). The NCs were characterized as non-homogenous colloidal system of injectable dosage form. This was reflected in SEM and TEM studies where the particles were aggregated. Remarkably, the morphological appearances in SEM and TEM were reflective of some differences. This might be due to the difference between the physical states of the samples analysed.

The NCs produced good antibacterial effects, with MICs of 4 to 8. In the present study, the spectrum of antibacterial potential of NCs against the screened organisms was increased, when compared to that of EG which has already been reported (Makeen et al., 2020). The results indicate that NC injectable formulation showed more efficacy than EG because of improved diffusion property. An important factor which is critical in bacterial cell targeting, i.e., EPR effect, is controlled by the size of the nanoparticles and ZP (Yang et al., 2007). The ZP and particle size of NCs indicate the readiness with which they diffuse across bacterial membranes. Thus, the diffusion of NCs into bacteria can be accomplished by optimizing the size of nanoparticles and surface charges. Anionic particles have been demonstrated to be less toxic than cationic NPs which can easily pass through the bacterial membrane pores. It has been reported that NPs of sizes of 50 to 200 nm readily permeate the bacterial membrane, making them very suitable for use in targeting (Tianmeng et al., 2014). Interestingly, the size of NCs prepared in the current research ranged from 100 – 200 nm, which indicate their suitability as injectable forms, as was reflected in antibacterial studies. Surprisingly, the efficacy of NC was found to have a wide range of action against Gram-positive and Gram-negative bacteria. When compared to normal ciprofloxacin at a concentration of 50 μg/mL, the effectiveness was nearly equal. On other hand the NC failed to block the proliferation of MCF-7 breast cancer cells ATCC even up to 300 μg / mL concentration and proving the lack of cytotoxicity effect indicating that not useful for treating against cancer. However, it is mandatory to screen further for cytotoxicity profiles against various human cell line, which is under progress as future studies. On the other hand, the NC failed to inhibit the proliferation of MCF-7 breast cancer cells ATCC even at concentrations as high as 300 μg / mL, demonstrating a lack of cytotoxicity and proving that it is ineffective in the treatment of cancer. However, it is necessary to screen further for cytotoxicity profiles against a variety of human cell lines, which is now being carried out as part of future research.

5. Conclusion

The present study revealed that injectable nanocrystals can be significantly formulated using natural exudate gel from *C. retrospiciens*, a desert plant widespread in Saudi Arabia. The research results indicate that nanocrystals have beneficial potential for use in producing new antibacterial drugs. Thus, the development of novel antibacterial agents will benefit human society by improving human health care. However, further studies are essential to standardize the formulation so as to develop an injectable nanocrystal dosage form.

CRediT Author Statement

M.H.S: Project administration and financial management; **S. M.S:** Conceptualization, experimentation, processing of results, writing and editing; **S.S.A:** SEM analysis and financial management; **H.A.M, Y.A, M.A:** Financial management and data collection; **O.S.M, A.Y.S:** Financial management and data collection; M.A.B: TEM analysis and financial management; **A.S:** Financial management and plant collection; **S.J. M:** Plant collection and processing. **S.M., M.E.E:** Experimentation. All authors have read and agreed to the published version of the manuscript.

Declaration of Competing Interest

The authors declare that they have no known competing financial interests or personal relationships that could have appeared to influence the work reported in this paper.

Acknowledgments

The authors extend their appreciation to the Deputyship for Research & Innovation, Ministry of Education in Saudi Arabia for funding this research work through the project number ISP20-13.

References

Aati, H., El-Gamal, A., Shaheen, H., Oliver, K., 2019. Traditional use of ethnomedicinal native plants in the Kingdom of Saudi Arabia. J. Ethnobiol. Ethnomedicine 15 (2). https://doi.org/10.1186/s13002-018-0263-2.

Alghamdi, M.A., Abdel, G.A.M., Alfahaid, F., Albshabshe, A., 2018. Herbal medicine use by Saudi patients with chronic diseases: across-sectional study (experience from Southern Regio of SaudiArabia). J. Health Spec. 6, 77–81. https://doi.org/10.4103/jhs.JHS_157_17.

Ayukekbong, J.A., Ntemgwa, M., Atabe, A.N., 2017. The threat of antimicrobial resistance in de-veloping countries: causes and control strategies. Antimicrob. Resist. Infect. Control. 6, 47. https://doi.org/10.1186/s13756-017-0208-x.

Cappuccino, J.G., Sherman, N., 2014. Microbiology – A Laboratory Manual. Pearson Education Inc., USA.

Ernest, A.A., Elaine, L.F., David, W.T., 2013. The enhanced permeability retention effect: a new paradigm for drug targeting in infection. J. Antimicrob. Chemother. 68, 257–274. https://doi.org/10.1093/jac/dks379.

Ghulam, Y., Mushtaq, A., Shazia, S., Ahmed, S.A., Javid, H., Muhammad, Z., Shafiq Ur, R., 2015. Ethnobotany of medicinal plants in the thar desert (Sindh) of Pakistan. J. Ethnopharmacol. 163, 43–59. https://doi.org/10.1016/j.jep.2014.12.053.

Hosseinkhani, A., Maryam, F., Elahe, R., Mohammad, M.Z., 2017. An evidence-based review on wound healing herbal remedies from reports of traditional Persian medicine. J. Evid. Based Complementary Altern. Med. 22 (2), 334–343. https://doi.org/10.1177/2156587216654773.

Ito, T., Sun, L., Bevan, M.A., Crooks, R.M., 2004. Comparison of nanoparticle size and electropho-retic mobility measurements using a carbon-nanotube-based coulter counter, dynamic light scattering, transmission electron microscopy, and phase analysis light scattering. Langmuir 20 (16), 6940–6945. https://doi.org/10.1021/la049524t.

Makeen, H.A., Santhosh J.M., Sivakumar, S.M., Saad Saeed, A., Ziaur, R., Md Shamsher., A., Syam, M., Mohammed, A., 2020. Documentation of bioactive principles of the exudate gel (EG)from the stem of Caralluma retrospiciens (Ehrenb) and in vitroantibacterial activity – Part A. Arab. J. Chem., 31, 6672-6681. 10.1016/j.arabjc.2020.06.022

Moni, S.S., Alam, M.F., Safhi, M.M., Jabeen, A., Sanobar, S., Siddiqui, R., Moochikkal, R., 2018. Potency of nano-antibacterial formulation from Sargassum binderi against selected human pathogenic bacteria. Braz. J. Pharm. Sci. 54, (4). https://doi.org/10.1590/s2175-97902018000417811 e17811.

Osama, A.M., Sivakumar, S.M., Muhammad, H.S., Haitham, A.B., Mohammed, G., Nabil, A.A., Abdulkarim, M.M., Saeed, A., Saad, S.A., Mohammed Ali, B., Intakhab Alam, M., Mohamed, E.E., 2021. Formulation and evaluation of injectable dextran sulfate sodium nanoparticles as a potent antibacterial agent. Sci. Rep. 11, 9914. https://doi.org/10.1038/s41598-021-89330-0.

Patra, J.K., Das, G., Fraceto, L.F., Estefania, V.R.C., Maria del Pilar, R.T., Laura Susana, A.T., Luis Armando, D.T., Renato, G., Mallappa, K.S., Shivesh, S., Solomon, H., Han-Seung, S., 2018. Nano based drug delivery systems: recent developments and future prospects. J Nanobi-otechnol 16, 71. https://doi.org/10.1186/s12951-018-0392-8.

Saad, S.A., Hafiz, A.M., Santhosh, J.M., Sivakumar, S.M., 2020. Documentation of bioactive prin-ciples of the flower from Caralluma retrospiciens (Ehrenb) and in vitro antibacterial activi-ty – Part B. Arab. J. Chem. 13 (10), 7370–7377. https://doi.org/10.1016/j.arabjc.2020.07.023.

Sivakumar, S.M., Mohammad, F.A., Mohammed, M.S., Muhammad, H.S., Hafiz, A.M., Mohamed, E.E., 2020. Development of formulation methods and physical characterization of injectable sodium selenite nanoparticles for the delivery of sorafenib tosylate. Curr. Pharm. Biotechnol. 21 (8). https://doi.org/10.2174/1389201021666191230124041.

Sultan, M.H., Alanazi, A.Z., Sivakumar, S.M., Saeed, A., Saad, S.A., Osama, A.M., Mohamed, E.E., 2020. Bioactive Principles and Potentiality of Hot Methanolic Extract of the Leaves from Artemisia absinthium L "in vitro Cytotoxicity Against Human MCF-7 Breast Cancer Cells, Antibacterial Study and Wound Healing Activity". Curr. Pharm. Biotechnol. 21 (15), 1711–1721. https://doi.org/10.2174/1389201021666200928150519.

Tianmeng, S., Yu Shrike, Z., Bo, P., Dong, C.H., Miaoxin, Y., Younan, X., 2014. Engineered nanoparticles for drug delivery in cancer therapy. Angew. Chem. 53, 12320–12364. https://doi.org/10.1002/anie.201403036.

Wided, N. M., Robert, D. A., Brian, S.C., 2021. Safe Nanoparticles: Are We There Yet?. Int. J. Mol. Sci., 2021, 22(1), 385. 10.3390/ijms22010385

Yang, J., Lee, J.Y., Too, H.P., 2007. A general phase transfer protocol for synthesizing alkaline sta-bilized nanoparticles of noble metals. Anal. Chim. Acta. 588 (1), 34–41. https://doi.org/10.1016/j.aca.2007.01.061.